Colloidal Synthesis of Halide Perovskite Semiconductor Nanocrystals/Quantum Dots and Their Optoelectronic Properties

M.Sc. Thesis

By

Aviral Upadhyay

(Roll Number: 2303151009)



Under the guidance of

Dr. Onkar S. Game

Department of Physics

Indian Institute of Technology Indore

May 2025

Colloidal Synthesis of Halide Perovskite Semiconductor Nanocrystals/Quantum Dots and Their Optoelectronic Properties

A THESIS

Submitted in partial fulfillment of the requirements for the award of the degree

of

Master of Science

By
Aviral Upadhyay

(Roll Number: 2303151009)



Department of Physics

Indian Institute of Technology Indore

May 2025



INDIAN INSTITUTE OF TECHNOLOGY INDORE

CANDIDATE'S DECLARATION

I hereby certify that the work which is being presented in the thesis entitled Colloidal Synthesis of Halide Perovskite Semiconductor Nanocrystals/Quantum Dots and Their Optoelectronic Properties in the partial fulfillment of the requirements for the award of the degree of MASTER OF SCIENCE and submitted in the DEPARTMENT OF PHYSICS, Indian Institute of Technology Indore, is an authentic record of my own work carried out during the time period from August 2023 to May 2025 under the supervision of Dr. Onkar S. Game, Assistant Professor, Department of Physics, IIT Indore.

The matter presented in this thesis has not been submitted by me for the award of any other degree of this or any other institute.

of this of any other institute.	Hylled 20/05/25 Signature of the student with date
	(Aviral Upadhyay)
This is to certify that the above statement made by the knowledge.	candidate is correct to the best of my/our
	989ame
	Signature of the Supervisor of
	M.Sc. thesis (with date)
	(Dr. Onkar S. Game)
Aviral Upadhyay has successfully given his M.Sc. C	Oral Examination held on May 2025 .
	21-05-25 Signature of DPGC Convener (with date)

(DPGC Convener)

Acknowledgment

I would like to express my heartfelt gratitude to my supervisor Dr. Onkar S Game. His continuous support, guidance, and encouragement were important throughout the course of my MSc. project. His insightful feedback and unwavering mentorship have been instrumental not only in the successful completion of this work but also in shaping my academic journey.

I also sincerely appreciate Dr.Rupesh S. Devan and his research group, Nano-architecture Research Group (NRG) from the MEMS Department at IIT Indore for granting me access to their labs for experiments. Special thanks to Department of Biosciences & Biomedical Engineering and Department of Chemistry for extending access to the TCSPC and PL facility, as well as to the SIC central facility. My appreciation extends to my fellow lab mates from Advanced Energy Material and Devices (AEMD) research group. I would like to thank Ms.Aayushi Miglani and my friend Vaibhav Pratap Singh for their valuable assistance during my project.

Finally, I thank my parents and family for their unconditional love and support that kept me going throughout this academic journey.

Abstract

Halide perovskite quantum dots (QDs) have gained attention as potential materials for optoelectronics and quantum photonics applications due to their adjustable band gap, high photoluminescence quantum yield (PLQY), narrow emission, and facile synthesis. Here, we have focused on colloidal synthesis and characterization of cesium lead bromide (CsPbBr₃) QDs, and optimization of reaction parameters to study and analyse their optoelectronic properties. The quantum dots were synthesized using the ligand-assisted reprecipitation (LARP) technique, employing oleylamine (OLA) and oleic acid (OA) as organic ligands to control the nucleation and growth stages of the crystal formation. Synthesis was carried out at different temperatures. We have studied the effect of varying synthesis temperature, changing reaction environment, and injection method on its optical properties. We have used characterization techniques like UV-Vis and Photoluminescence (PL) spectroscopy, and Time-Correlated Single Photon Counting (TCSPC) to analyze the absorption wavelength, fluorescence lifetime, emission wavelength, and spatially resolved photoluminescence images. We applied the Brus model, a theoretical framework, in conjunction with experimental measurements to determine the size of the synthesized nanocrystals. By optimizing the synthesis process, we obtained quantum dots with size less than 5 nm, having high photoluminescence intensity, large Stokes shift (105 nm), and excitonic lifetime (in ns) that will be suitable for LEDs and quantum emitter applications. These results showed the potential of CsPbBr₃ QDs as stable, efficient, and tunable light sources for their applications and integration into photonic devices.

Contents

1	Intr	oductio	n	5
	1.1	Histori	ical context	5
	1.2	Colloid	dal quantum dots (CQDs)	6
		1.2.1	Halide perovskite quantum dots	6
2	The	oretical	framework	9
	2.1	Brus n	nodel	9
	2.2	Appro	ximation for the model	10
	2.3	Calcul	ation of band gap energy of quantum dot	10
		2.3.1	Calculation	10
		2.3.2	Electron-Hole Pair Hamiltonian	11
		2.3.3	Quantum Dot Band Gap	12
		2.3.4	Definitions	12
	2.4	Deduc	tions from Brus Model	13
3	Met	hodolog	gy	14
	3.1	Supers	saturated Recrystallization	14
	3.2	Experi	mental Section	14
		3.2.1	Parameter Variation in CsPbBr ₃ Quantum Dot Synthesis	15
		3.2.2	Synthesis Protocol	15
		3.2.3	Purification	17
	3.3	Data c	ollection methods	17
		3.3.1	Ultraviolet-Visible (UV-Vis) Spectroscopy	17
		3.3.2	Photoluminescence (PL) Spectroscopy	18
		3.3.3	Time Correlated Single Photon Counting (TCSPC)	18

	3.4	Analyt	ical Approach	19
4	Resu	ults and	Discussion	20
	4.1	Experi	mental results	20
		4.1.1	Optical images of CQDs	20
		4.1.2	UV-Vis Spectroscopy results	21
		4.1.3	Photoluminescence (PL) spectroscopy results	23
		4.1.4	Time Correlated Single Photon Counting (TCSPC) results	24
	4.2	Theore	etical calculations	25
		4.2.1	Band Gap and Quantum Dot Size Estimation	25
5	Con	clusion		28

List of Figures

1.1	Perovskite structure [7]	6
1.2	Structures of CsPbX ₃ [12]	7
1.3	Schematic of the CsPbBr ₃ crystal structure. [16]	8
3.1	Representation of supersaturated crystallization or LARP [18]	16
3.2	Experimental setup for UV-Visible spectrometer	17
3.3	Experimental setup for fluorescence measurements	19
4.1	a) Prepared samples under a) no illumination, b) UV illumination	20
4.2	UV-Vis absorption spectra of CsPbBr ₃ quantum dots synthesized at 30°C and 70°C,	
	showing the first excitonic peak at approximately 415nm	21
4.3	UV-Vis absorption spectra of CsPbBr ₃ quantum dots synthesized by three different	
	injection methods DTU, UTD, and DBD showing the first excitonic peak at 416nm,	
	415nm, and 419nm respectively	22
4.4	UV-Vis absorption spectra of CsPbBr ₃ quantum dots synthesized under inert and am-	
	bient environment showing the first excitonic peak at 399nm and 417nm respectively.	22
4.5	PL spectra for 30°C, 70°C and inert sample showing emission at 508nm, 510nm, and	
	504nm respectively	23
4.6	Fitting parameters	24
4.7	Time-resolved PL decay curve	25
4.8	Combined Tauc and Brus plot for temperature variation	26
4.10	Combined Tauc and Brus plot for environment variation	26
4.9	Combined Tauc and Brus plot for injection method variation	27

List of Tables

1.1	Properties of CsPbBr ₃ perovskite QDs	8
4.1	Excitonic peak values under various synthesis conditions for CsPbBr ₃ QDs	23
4.2	Band gap and size under various synthesis conditions for CsPbBr ₃ QDs	27

Chapter 1

Introduction

1.1 Historical context

Herbert Frohlich, in 1937 studied the free electron gas model for metals and predicted that small particles should have size-dependent material properties [1].

In early 1980s, Alexey Ekimov [2] and Alexander Efros, were working on semiconductor doped glass at S.I. Vavilov State Optical Institute, to understand the structural, chemical and growth properties of colloidal particles in coloured glass. Ekimov produced copper chloride tinted glass and heats it at 500-700 degree Celsius over 1-96 hours, then by doing the X-ray analysis, he found that copper chloride crystals formed from size ranging 2-30nm. He observed that absorption lines were blue shifted for smaller crystals to nanocrystals that were as small as few nanometres. Ekimov observed this and attributed this as quantum size effects. Hence, Semiconductor quantum dots were discovered. In 1983, Louis Brus [3] [4] and his co-workers at Bell Labs were studying semiconductor particles in liquid colloids. While synthesizing CdS particles in a solution, they observed a major difference between freshly prepared particles and those that had been left to sit for several hours. Over time, the particles underwent growth, resulting in the formation of larger particles that absorbed light in same way the cadmium sulfide does, but the smaller particles showed a blue shift in their absorption spectrum. Brus attributed this difference between large and small particles as quantum size effects. In 1993, Moungi Bawendi' research group synthesized quantum dots by developing a method called hot-injection method [5]. They injected suitable precursors into a hot solvent having high boiling point, that led to the supersaturations of precursors followed by nucleation and growth. The growth is stopped by lowering the temperature of solvents suddenly, which will result in the formation of colloidal dispersion in which the particles can be selected by purifying and size dependent precipitation.

1.2 Colloidal quantum dots (CQDs)

CQDs (colloidal quantum dots) or semiconductor nanocrystals are tiny particles made of semiconductors, typically in the nanometre range, and are suspended in a liquid. CQDs have the same structure as their bulk counterparts, but their properties can be tailored by adjusting one factor: the particle's size.

1.2.1 Halide perovskite quantum dots

Halide perovskite

The crystal structure with stoichiometry ABX_3 consists of halide anions (such as Cl^- , Br^- , or I^-) occupying the X site, Group 1 monovalent alkali metals (such as cesium) or small organic cations (like formamidinium or methylammonium) occupying the A site, and divalent cations (such as Pb^{2+} or Sn^{2+}) occupying the B site. This structure has been considered a strong candidate for applications in photovoltaics and LEDs due to its high (PLQY), tunable band gap, and defect-tolerant nature. The structural stability of the perovskite structure is often evaluated using the tolerance factor, t. [6].

$$t = \frac{r_A + r_X}{\sqrt{2}(r_B + r_X)}$$

where r_X , r_B , and r_A are the ionic radii of the X, B, and A ions, respectively.

t will be 1 for ideal and stable structure. There is also a subgroup of perovskites, such as hybrid

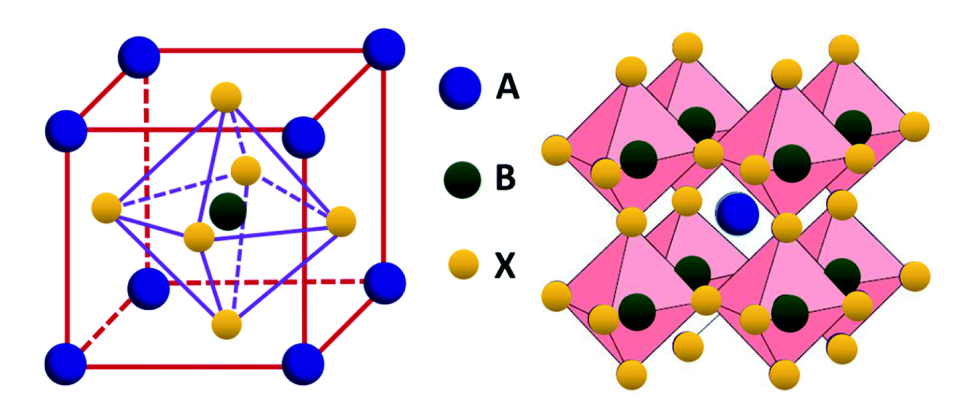


Figure 1.1: Perovskite structure [7]

organic-inorganic perovskites (e.g., methylammonium lead iodide, CH₃NH₃PbI₃) and all-inorganic

halide perovskites (e.g., cesium lead bromide, CsPbBr₃). The first report on hybrid organic-inorganic perovskites was published by schmidt [8]. Kovalenko's group later synthesized all-inorganic halide perovskite quantum dots (QDs) of CsPbX₃ using the hot-injection method [9].

Inorganic halide perovskite quantum dots (IHPQDs)

IHPQDs, with general formula $CsPbX_3$ (X = Cl, Br, I, or a mixture of halides such as Cl/Br or Br/I), are a class of materials in which the A site is typically occupied by an inorganic cation such as Cs (cesium), the B site by divalent cations like Pb^2 , and the X site by halide anions (Cl, Br, I, or their mixtures). Inorganic perovskites can exist in three structural phases: cubic, tetragonal, and orthorhombic [10]. Inorganic perovskite quantum dots (QDs) exhibit strong photoluminescence (PL)

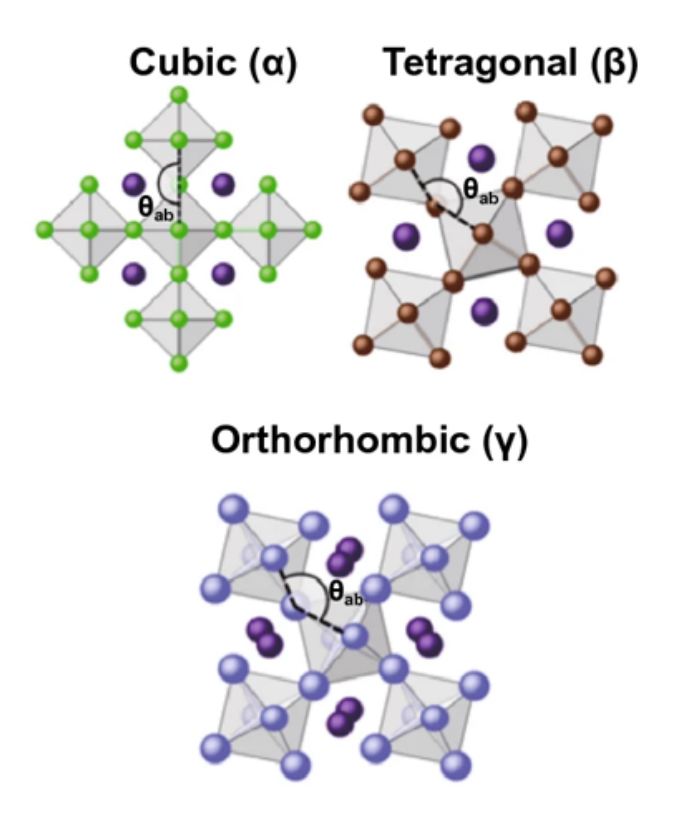


Figure 1.2: Structures of CsPbX₃ [12]

emission and can achieve photoluminescence quantum yields (PLQY) exceeding 99%. By varying the halide composition, the PL emission can be tuned across the entire visible spectrum. In 2015, Protesecu *et al.* demonstrated that the emission spectra of CsPbX₃ QDs can be tuned from 400 nm to 690 nm [9]. These unique optoelectronic properties make inorganic perovskite QDs highly promising candidates for applications in light-emitting devices, lasers, and other optoelectronic technologies. The synthesis methods of inorganic perovskite QDs can be broadly classified into two categories. The first is direct synthesis, which includes LARP, hot-injection, and chemical vapor deposition

(CVD) [11]. The second is post-synthesis modification, which uses pre-synthesized QDs as templates and includes approaches such as ion exchange and phase transformation [13].

CsPbBr₃

CsPbBr₃ inorganic QDs, having orthorhombic structure at room temperature, where each Pb²⁺ is bonded to 6 Br⁻ ions that forms PbBr₆ octahedra and each Cs⁺ is surrounded by 12 Br⁻ ions filling the cuboctahedral voids between PbBr₆ octahedra. Also CsPbBr₃ undergoes temperature-dependent structural phase transitions, transforming into tetragonal and cubic phases at elevated temperatures. These phase changes affect the lattice symmetry and electronic band structure, which in turn impact charge carrier dynamics and optical properties such as emission wavelength and intensity.

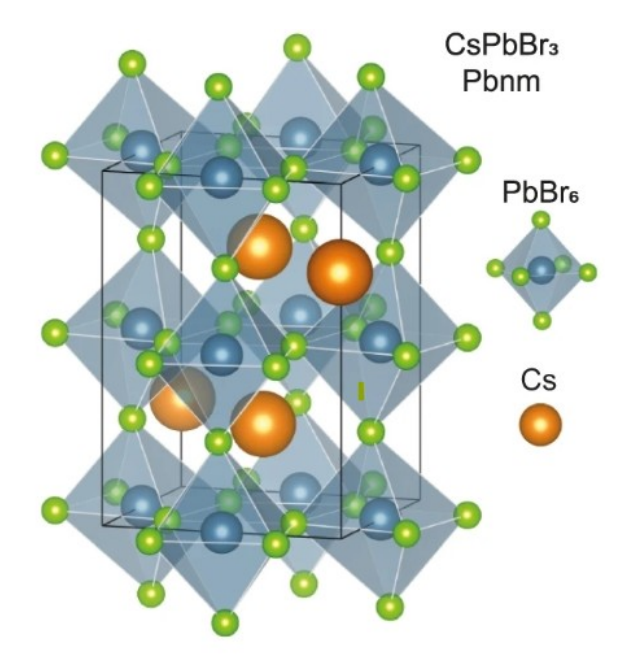


Figure 1.3: Schematic of the CsPbBr₃ crystal structure. [16]

Property	Description
Chemical formula	$CsPbBr_3$
Crystal structure	Orthorhombic
Tolerance factor	0.862
Bandgap	2.36 eV
Absorption spectrum	400–500 nm (blue-
	green region)
Photoluminescence	500–530 nm (tunable
spectrum	by size)
Bohr exciton radius	7 nm

Table 1.1: Properties of CsPbBr₃ perovskite QDs.

CsPbBr₃ has a direct band gap of 2.36 eV, which corresponds to green emission under UV illumination. The band edge energy of quantum dots can be adjusted by altering their size, a consequence of quantum confinement effects. The upper valence band of CsPbBr₃ has major contributions from the 4p⁶ orbitals of the Br anion and the 6s² orbitals of the Pb cation. The lower conduction band is mainly composed of the p orbitals of the Pb cation and the 4p⁶ orbitals of the Br anion. Therefore, when the halide changes, the energy of the Br site 4p⁶ orbitals changes, leading to variation in the band gap of perovskite quantum dots (PQDs) [14]. CsPbBr₃ QDs exhibit high photoluminescence quantum yields (often above 80%), short radiative lifetimes ranging from 1 to 29 ns, and carrier mobilities 2.1cm²/V·s [15], making them excellent candidates for optoelectronic devices.

Chapter 2

Theoretical framework

2.1 Brus model

The Brus model [3] [4] provides the first theoretical calculation of the emission energy of semiconductor quantum dots (QDs). This model employs the effective mass approximation, meaning that the masses of electrons and holes are modified to account for the periodic potential of the crystal lattice. Brus studied spherical semiconductor colloidal nanocrystals, using CdS and CdSe as examples.

The Brus equation describes the band gap energy of quantum dots, which corresponds to the energy required to create an electron-hole pair. When a quantum dot absorbs light, an electron is elevated from the valence band to the conduction band, resulting in the creation of a positively charged vacancy called a hole.

The Brus equation calculates the confinement energy, which is the energy needed to confine the electron-hole pair (exciton) within the quantum dot. His study showed that the emission energy has an inverse square dependence on the quantum dot radius.

The Brus equation is given as:

$$E(R) = E_g(bulk) + \frac{h^2 \pi^2}{2R^2} \left(\frac{1}{m_h^*} + \frac{1}{m_e^*} \right) - \frac{1.8e^2}{4\pi \varepsilon R}$$

where E_g is the bulk band gap energy, R is the quantum dot radius, m_h^* and m_e^* are the effective masses of the hole and electron respectively, ε is the dielectric constant of the material, e is the elementary charge, and h is Planck's constant.

2.2 Approximation for the model

- 1. In his model, Brus considered a spherical nanocrystal of radius a.
- The only charges present within the nanocrystal are the excited electron and hole; all other bound electrons are neglected. This simplifies the system by assuming that no other point charges exist within the nanocrystal.
- 3. The potential energy at the boundary and outside the nanocrystal is assumed to be infinite. Consequently, both electron and hole are strictly confined within the nanocrystal. Due to this infinite potential at the boundary, the system is analogous to a particle in a spherical infinite potential well (spherical box).

2.3 Calculation of band gap energy of quantum dot

We will take cadmium selenide (CdSe) as our example. First, we consider the Hamiltonian for a free point charge [17]. By solving the Schrödinger equation in a spherically symmetric potential, we obtain the corresponding wavefunctions and energy levels.

We then analyze a system comprising both an electron and a hole confined within a spherically symmetric potential. The corresponding Hamiltonian accounts for the kinetic energies of the individual charge carriers and incorporates the Coulomb interaction between them.

Using an uncorrelated product wavefunction as an approximation, we substitute it into the Schrödinger equation to obtain the total energy of the lowest-energy exciton. This energy corresponds to the quantum dot band gap and includes contributions from both quantum confinement and Coulombic effects.

2.3.1 Calculation

Consider a spherical particle of radius a with an infinitely high potential barrier surrounding the sphere. The potential is given by:

$$V(r) = \begin{cases} 0, & r < a \\ \infty, & r \ge a \end{cases}$$

The Hamiltonian describing a free point charge (either an electron or a hole) within a nanocrystal is given by:

$$H = -\frac{\hbar^2}{8\pi^2 m_c^*} \nabla_c^2 + V(r)$$
 (2.1)

where m_c^* denotes the effective mass of the charge carrier, while r represents the radial distance from the center of the nanocrystal.

The wavefunction of the electron and hole in a spherically symmetric infinite potential well is:

$$\psi_{n,l,m}^{e,h}(r) = \sqrt{\frac{2}{a^3}} \cdot \frac{j_l\left(\frac{\phi_{l,n}r}{a}\right)}{j_{l+1}(\phi_{l,n})} Y_{l,m}(\theta,\varphi)$$
(2.2)

where:

- $j_l\left(\frac{\phi_{l,n}r}{a}\right)$ is the spherical Bessel function of order l
- $\phi_{l,n}$ is the *n*-th root of the spherical Bessel function
- a is the radius of the spherical box

The energy levels for the electron and hole in this system are:

$$E_{n,l} = \frac{\hbar^2 \phi_{l,n}^2}{2m_{e,h}^* a^2} \tag{2.3}$$

The corresponding ground state wavefunction and energy are:

$$\psi_n(r) = \frac{1}{r\sqrt{2\pi a}} \sin\left(\frac{n\pi r}{a}\right), \quad E_n = \frac{\hbar^2 n^2 \pi^2}{2m_c a^2}$$

2.3.2 Electron-Hole Pair Hamiltonian

For an electron-hole pair confined in the same potential, the Hamiltonian is:

$$H = -\frac{\hbar^2}{8\pi^2} \left(\frac{1}{m_e^*} \nabla_e^2 + \frac{1}{m_h^*} \nabla_h^2 \right) - \frac{e^2}{4\pi\varepsilon |r_e - r_h|}$$
 (2.4)

where r_e and r_h are the positions of the electron and hole respectively, and the last term represents the Coulomb attraction between them.

To determine the lowest energy of the system, we use the individual lowest-energy wavefunctions ψ_e

and ψ_h . Assuming an uncorrelated product wavefunction:

$$\phi(r_e, r_h) = \psi_1(r_e)\psi_1(r_h) \tag{2.5}$$

Substituting into the Schrödinger equation:

$$H\phi(r_e, r_h) = E\phi(r_e, r_h) \tag{2.6}$$

$$\Rightarrow \left[-\frac{\hbar^2}{8\pi^2 m_e^*} \nabla_e^2 - \frac{\hbar^2}{8\pi^2 m_h^*} \nabla_h^2 - \frac{e^2}{4\pi\varepsilon (r_e - r_h)} \right] \psi_1(r_e) \psi_1(r_h) = E \psi_1(r_e) \psi_1(r_h)$$
 (2.7)

Using this approach, the energy of the exciton is given by:

$$E = \frac{\hbar^2 \pi^2}{2a^2} \left(\frac{1}{m_e^*} + \frac{1}{m_h^*} \right) - \frac{e^2}{4\pi \varepsilon_{\text{CdSe}} \varepsilon_0 (r_e - r_h)}$$
 (2.8)

2.3.3 Quantum Dot Band Gap

The total transition energy or the band gap of the quantum dot, including quantum confinement and Coulombic effects, is:

$$E_g(QD) = E_{tr} = E_g(bulk) + \frac{\hbar^2 \pi^2}{2\mu a^2} - \frac{e^2}{4\pi\varepsilon_{CdSe}\varepsilon_0(r_e - r_h)}$$
(2.9)

where μ is the reduced mass:

$$\mu = \frac{m_e^* m_h^*}{m_e^* + m_h^*} \tag{2.10}$$

Considering CdSe as an example and using the approximation:

$$r_e - r_h = \frac{a}{1.8} \tag{2.11}$$

we get:

$$E_g(QD) = E_{tr} = E_g(bulk) + \frac{\hbar^2 \pi^2}{2\mu a^2} - \frac{1.8e^2}{4\pi \varepsilon_{CdSe} \varepsilon_0 a}$$
 (2.12)

2.3.4 Definitions

• $E_g(QD)$: Band gap energy of the quantum dot

- E_g (bulk): Band gap energy of the bulk semiconductor
- E_{tr} : Transition energy
- ε_0 : Vacuum permittivity
- $\varepsilon_{\text{CdSe}}$: Dielectric constant of CdSe

Note: The polarization energy has been neglected, as it is negligible in comparison to the kinetic and Coulomb energies.

2.4 Deductions from Brus Model

- 1. Brus equation shows that confinement energy has inverse dependence on square of radius of spherical semiconductor nanocrystal.
- 2. Confinement energy we get is basically the energy of two particles in one box.
- 3. For large crystal, the value of the transition energy predicted by the Brus model matches the experimental value, but it deviates from experimental value for small crystal.
- 4. Brus model did not account for electron-hole spatial correlation effect.

Chapter 3

Methodology

3.1 Supersaturated Recrystallization

Ligand assisted reprecipitation or supersaturated recrystallization method is used for the synthesis of quantum dots.

Supersaturated recrystallization involves transfer of inorganic ions from a very good solvent into very bad solvent. This process involves mixing or dissolving the inorganic ions into a solvent in which their concentrations are smaller than their solubilities so they will be dissolved without crystallization. When this solution will attain equilibrium state then transfer this solution into a poor solvent. So it will be in nonequilibrium state of supersaturation and then by varying the temperature, adding a solvent, precipitation and crystallization reactions takes place and system will attain equilibrium state. This process is also called "Ligand assisted reprecipitation" (LARP), when it involves the presence of ligands that help the formation and growth of crystals. This method of synthesis is carried out in normal room temperature environment without the need of any inert gas, unlike hot injection method which requires high temperature and inert atmosphere.

3.2 Experimental Section

Synthesis of CsPbBr₃ Quantum dots/nanocrystals, which is an inorganic perovskite nanocrystal, was carried out by using supersaturated recrystallization method [18]. In this Supersaturated Recrystallization synthesis, various inorganic ions are transferred from a good solvent to a poor solvent.

Our first task is to select precursor salts for Cesium and Lead, followed by suitable ligands to control

the kinetics of the reaction, and suitable solvents for the reaction to take place. Here we will choose

CsBr (cesium bromide) and PbBr₂ (lead (II) bromide) as ion sources, and Dimethylformamide (DMF) or Dimethyl sulfoxide (DMSO) as good solvents. Then Oleylamine (OAm) and Oleic acid (OA) are selected as surface ligands, and toluene is used as the poor solvent.

As soon as the precursor solution was dropped into toluene, strong green colour emission was observed under UV light illumination, confirming the formation of CsPbBr₃ QDs. By changing PbX₂ and CsX compositions and the method of injection of precursor, many different samples can be prepared.

3.2.1 Parameter Variation in CsPbBr₃ Quantum Dot Synthesis

We have synthesized various samples by altering different parameters that can control the reaction.

These are:

- Temperature variation: To understand the impact of synthesis temperature on the optoelectronic properties of QDs, synthesis were done under two different thermal conditions. Samples were synthesized at room temperature (30°C) and at elevated temperature (70°C) to study how synthesis temperature affects nucleation and growth phase of crystals.
- **Injection method variation:** Samples were synthesized by controlling the speed and direction of injection of precursor into antisolvent. Two categories of sample were synthesized here: one where the injection is done in a burst mode while changing the direction from up to down and vice versa, and second where the injection is done by drop-by-drop method.
- Environment variation: To study the effect of environment on nucleation and growth of nanocrystals. Samples were synthesized under two different environmental conditions: ambient atmosphere (air) and an inert atmosphere (nitrogen). This comparison aims to explore how the presence or absence of oxygen and moisture influences the crystallization process, surface passivation, and ultimately the structural and optoelectronic properties of the resulting quantum dots (QDs).

3.2.2 Synthesis Protocol

1. **Preparation of lead precursor solution:** Cesium bromide (CsBr) and lead(II) bromide (PbBr₂) were selected as precursor salts for the synthesis [19]. They were weighted and collected

in clean glass vials. Then a suitable good polar solvent like Dimethylformamide (DMF) or Dimethylsulfoxide (DMSO) was then measured and added into the vials in which precursor salts were weighted. The polar solvents will help in effectively dissolving the metal halide salts. In addition to the precursor salts and solvent, organic ligands—oleic acid (OA) and oley-lamine (OAm)—were added to the solution. These long-chain ligands are essential for surface passivation of the nanocrystals, helping to prevent aggregation and regulate their growth throughout the synthesis process. The mixtures were subjected to continuous stirring until complete salts is dissolved that lead to clear and homogeneous lead precursor solution.

2. Antisolvent solution: Antisolvent is measured carefully and collected in a separate glass vial. The choice of antisolvent—typically a nonpolar solvent such as toluene, hexane, or chloroform was based on its ability to induce rapid precipitation of nanocrystals upon mixing with the polar precursor solution. The antisolvent was kept at room temperature and was either left undisturbed or subjected to mild stirring prior to the injection step depending upon the synhtesis protocol.

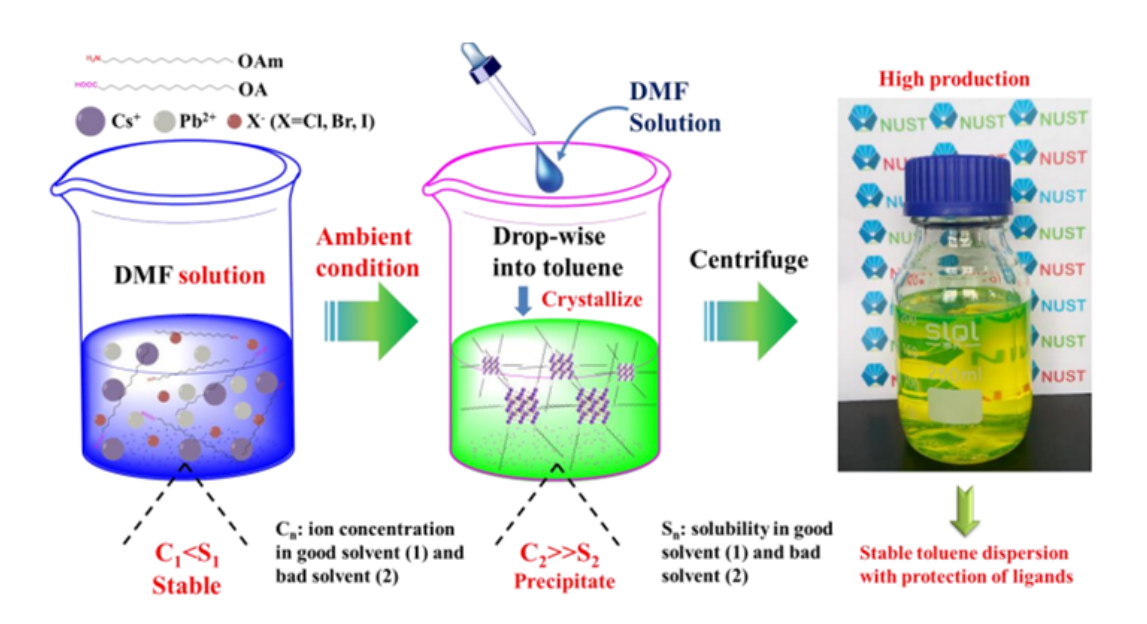


Figure 3.1: Representation of supersaturated crystallization or LARP [18]

3. **Synthesis of CsPbBr₃ Quantum dots:** The precursor solution containing dissolved CsBr, PbBr₂ and surface ligands (oleic acid and oleylamine) in a polar solvent such as DMF or DMSO, was injected into a vigorously stirred nonpolar antisolvent—typically toluene—at room temperature. Upon injection, rapid nucleation and subsequent growth of nanocrystals were triggered due to the sudden decrease in solubility, leading to the formation of CsPbBr₃

quantum dots (QDs). Strong green colour emission was observed under UV light illumination confirming the formation of CsPbBr₃ QDs.

3.2.3 Purification

After the synthesis, the quantum dots are purified through several rounds of centrifugation. After each round, the supernatant is carefully extracted from the centrifuge tubes and transferred into separate vials. These purified samples are then ready for various characterization techniques, which will confirm and validate the successful synthesis of quantum dots.

3.3 Data collection methods

After synthesizing CsPbBr₃ QDs/nanocrystals, we have performed different characterization techniques on the prepared samples to know about its different properties.

3.3.1 Ultraviolet-Visible (UV-Vis) Spectroscopy

In this spectroscopy technique, UV and visible light are used to illuminate the sample that we want to study. When the sample is illuminated with UV-Vis light, several processes can occur: reflection, absorption, and transmission. This technique is used to estimate the band gap of a material with the help of an absorbance vs. wavelength plot. Absorbance is defined as the amount of light that gets absorbed by the sample.

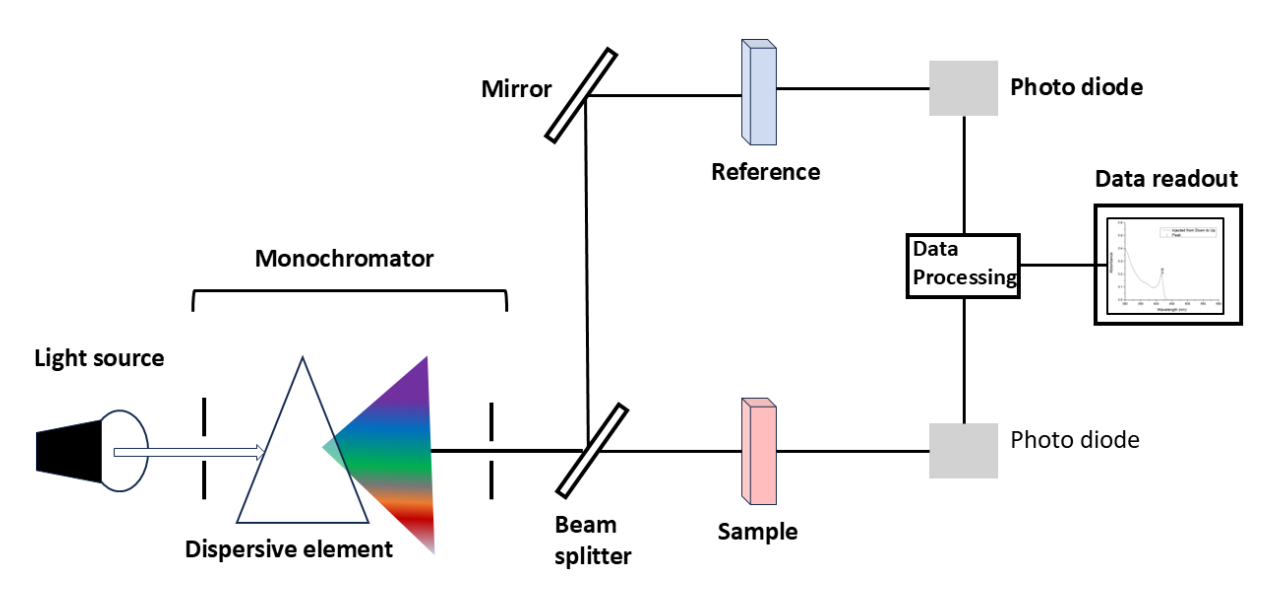


Figure 3.2: Experimental setup for UV-Visible spectrometer

The Beer-Lambert law quantifies the relationship between absorbance, light path length, and solute concentration, where absorbance is directly proportional to both.

$$A = \epsilon cd \tag{3.1}$$

Where:

- A = absorbance (arbitrary units)
- ϵ = extinction coefficient
- c =concentration of the solution
- d = path length of the sample (in cm)

In the context of colloidal quantum dots, we illuminate the sample and then check at which wavelength the absorbance (defined as the negative logarithm of transmittance) is maximum, which shows the sample is absorbing light at that particular wavelength. [Setup image]

3.3.2 Photoluminescence (PL) Spectroscopy

It is a non-destructive spectroscopy technique that is employed to investigate the electronic and optical characteristics of materials. Upon laser illumination, electrons in the valence band are promoted to the conduction band, leading to the generation of electron-hole pairs, referred to as excitons. When electrons and holes recombine, the sample emits photons, which are collected and analyzed in the PL spectrum. Spectral position and intensity obtained from this technique can provide information regarding band gap energy, exciton dynamics, quantum confinement effects, and defect states. In the context of quantum dots, with the help of this spectroscopy, we can find out band gap energy of QDs, quantum efficiency, and Stokes shift.

3.3.3 Time Correlated Single Photon Counting (TCSPC)

This technique is used to measure the time that a molecule/atom remains in the excited state when it is excited by an excitation pulse [20]. The idea is to measure the time delay between excitation (initiated by excitation pulse) and emission by a fluorescence detector that is kept at right angle to the sample. When the process of excitation and emission is repeated million times the electronics

attached to the system generate data which is a histogram of intensity versus time (in ns). We then fit the curve to extract the fluorescence lifetime of the sample.

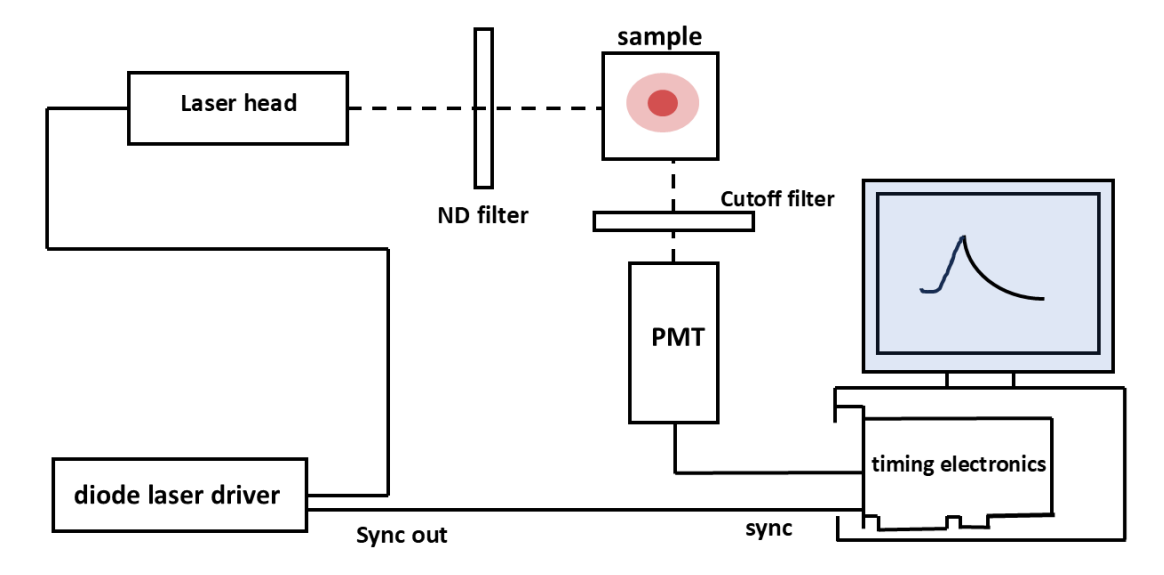


Figure 3.3: Experimental setup for fluorescence measurements

In the context of colloidal quantum dots, it is used to measure fluorescence lifetime that gives the information about the time the QDs will take to emit out photons after being excited.

3.4 Analytical Approach

To analyze the data obtained from different spectroscopic techniques, an analytical approach is used to evaluate the optical and electrical properties of quantum dots. UV-Vis spectroscopy was used to determine the excitonic peak and the onset of absorption, which was then analyzed using Tauc plot to estimate the band gap. The Brus equation, which gives the emission energy of quantum dot, was used to estimate quantum dot size by using band gap shifts. Photoluminescence spectra was used to extract emission peaks positions. TCSPC measurements were done to obtain time resolved emission which is then fitted with double exponentials to find radiative lifetimes.

All data processing and fitting were done using OriginPro 9.0 and Python. This multi-dimensional analytical framework provides a detailed understanding of size-dependent optical behaviour of CsPbBr₃ quantum dots.

Chapter 4

Results and Discussion

In this chapter, we will discuss the results obtained from our experiments. We present the experimental findings and further analyze them by integrating theoretical models with the experimental data.

4.1 Experimental results

4.1.1 Optical images of CQDs

Prepared samples of Colloidal Quantum Dots are illuminated under UV-light (wavelength 380nm) and they show emission as blue-greenish colour.

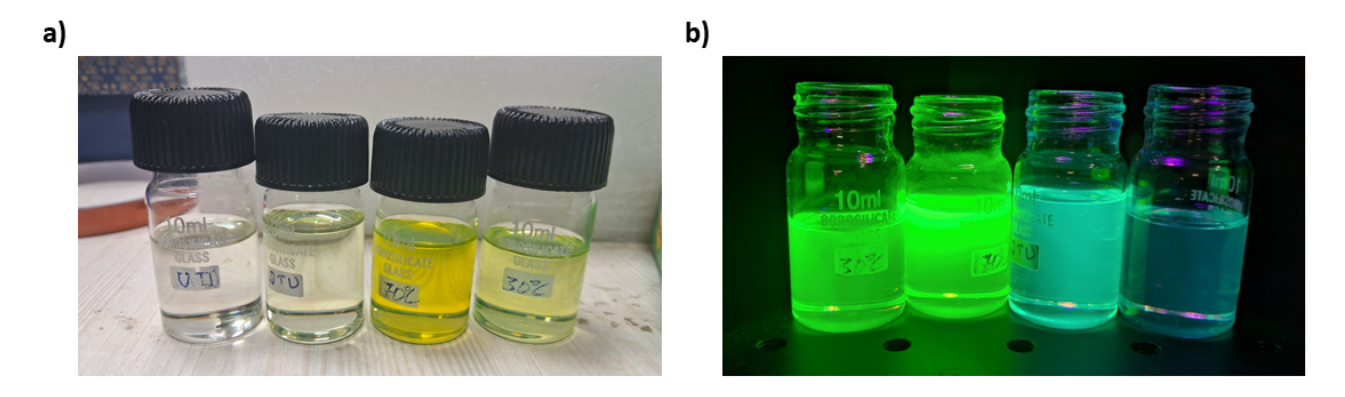


Figure 4.1: a) Prepared samples under a) no illumination, b) UV illumination

4.1.2 UV-Vis Spectroscopy results

Temperature variation

CsPbBr₃ quantum dots were synthesized at two different temperatures: 30°C and 70°C. The absorption spectra of both samples showed first excitonic absorption peak at 415nm, indicating similar quantum confinement effects and suggesting comparable particle sizes in both cases.

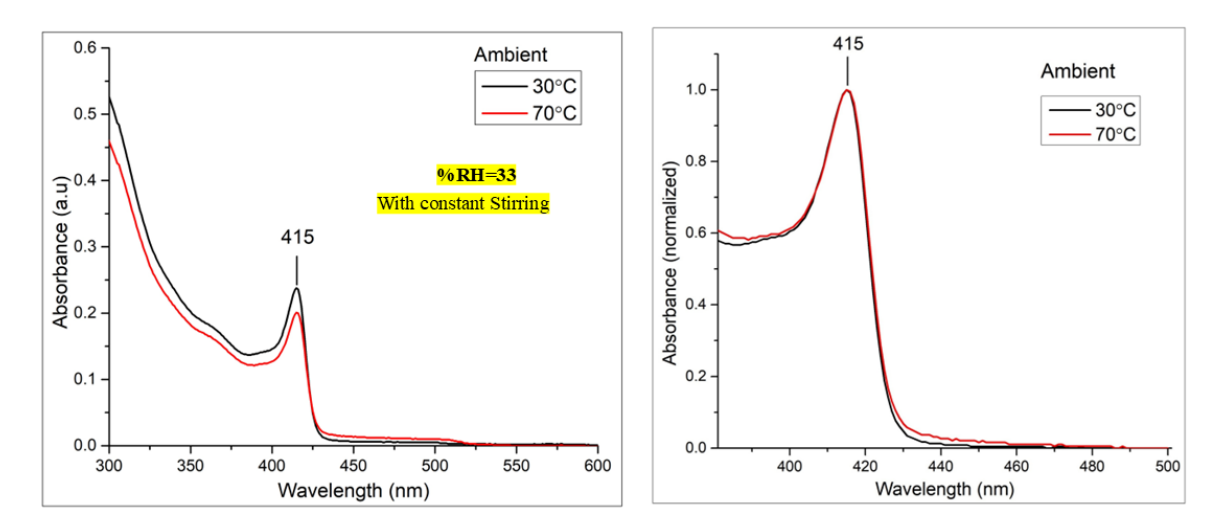


Figure 4.2: UV-Vis absorption spectra of CsPbBr₃ quantum dots synthesized at 30°C and 70°C, showing the first excitonic peak at approximately 415nm.

However, a slight variation was observed in the intensity of the absorption peaks. The sample synthesized at 30°C exhibited a marginally higher absorbance at the excitonic peak compared to the one synthesized at 70°C. This difference in absorbance may be attributed to variations in concentration, surface passivation, or optical density of the colloidal solutions, while the unchanged peak position indicates that the core structure and size of the quantum dots remained largely unaffected by the synthesis temperature within this range.

Injection method variation

We investigated the effect of different precursor injection methods on the optical properties of CsPbBr₃ quantum dots. The methods used were:

- Down-to-up (burst injection)
- Up-to-down (burst injection)

• Drop-by-drop injection

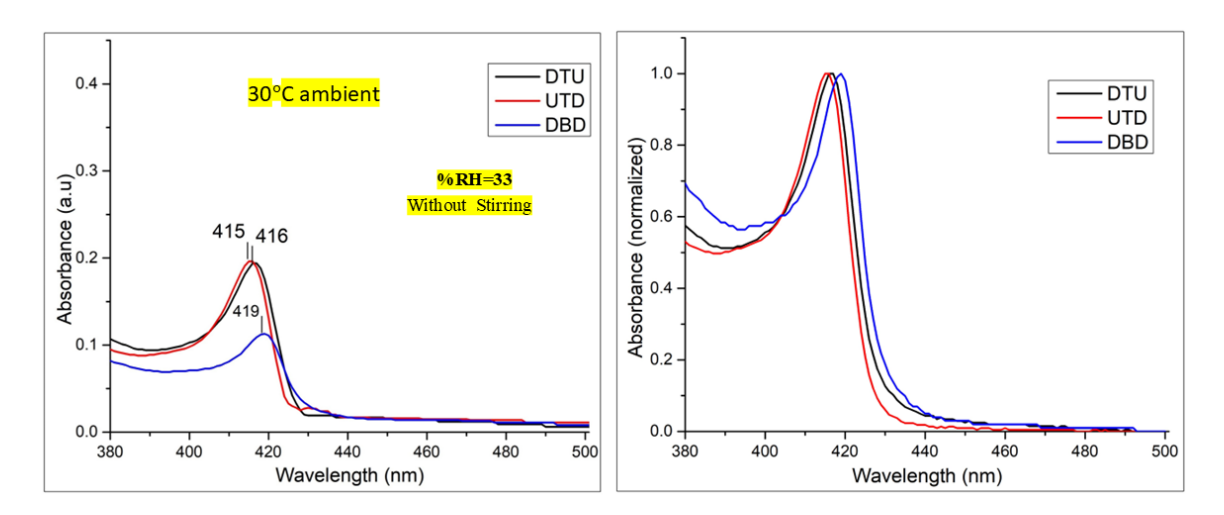


Figure 4.3: UV-Vis absorption spectra of CsPbBr₃ quantum dots synthesized by three different injection methods DTU, UTD, and DBD showing the first excitonic peak at 416nm, 415nm, and 419nm respectively.

The corresponding first excitonic absorption peaks were observed at approximately 416 for the down-to-up method, 415 for the up-to-down method, and 419 for the drop-by-drop method. These slight variations in peak position suggest that the injection technique can influence the nucleation and growth dynamics, thereby affecting the quantum dot size and optical properties.

Environment variation

We conducted further investigation into the impact of the synthesis environment on the optical characteristics of CsPbBr₃ quantum dots.

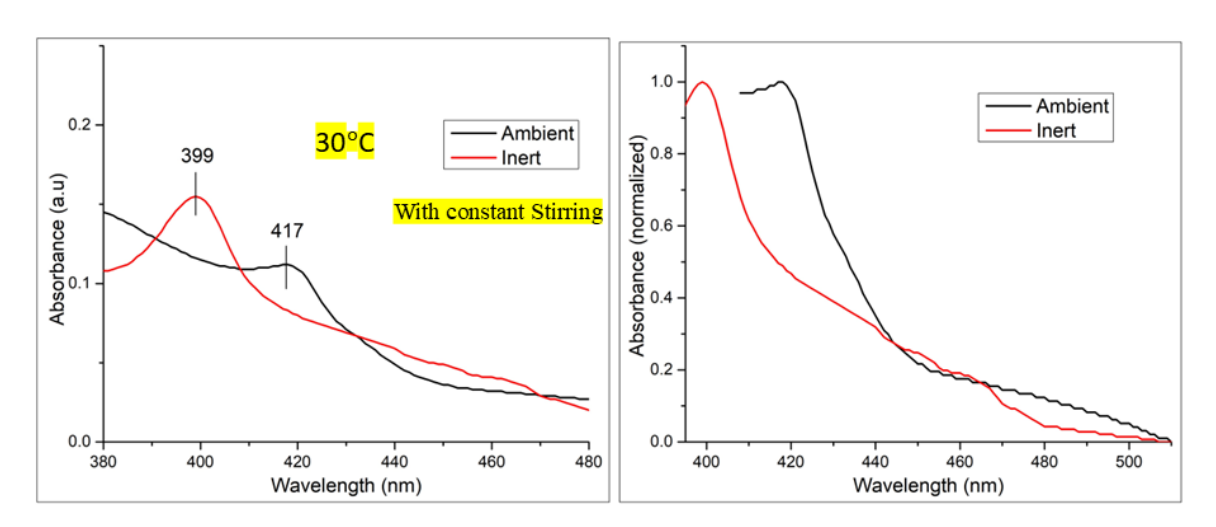


Figure 4.4: UV-Vis absorption spectra of CsPbBr₃ quantum dots synthesized under inert and ambient environment showing the first excitonic peak at 399nm and 417nm respectively.

The synthesis were done under two environment: inert and ambient conditions. The excitonic peak was observed at 417nm for ambient condition and 399nm for inert conditions. This shift suggests a possible difference in quantum dot size and surface defects influenced by synthesis environment that affect the growth process of these nanocrystals.

Parameter Type	Sample Description	Excitonic Peak (nm)
Temperature Variation	Sample T1 (30°C)	415
	Sample T2 (70°C)	415
Injection Method Variation	Sample I1 (Burst: Up to Down)	415
	Sample I2 (Burst: Down to Up)	416
	Sample I3 (Drop-by-Drop)	419
Environment Variation	Sample E1 (Ambient)	417
	Sample E2 (Inert: Nitrogen)	399

Table 4.1: Excitonic peak values under various synthesis conditions for CsPbBr₃ QDs.

4.1.3 Photoluminescence (PL) spectroscopy results

Photoluminescence (PL) spectroscopy was conducted to further analyze the optical properties of the CsPbBr₃ quantum dots synthesized under different conditions. The sample synthesized at 30

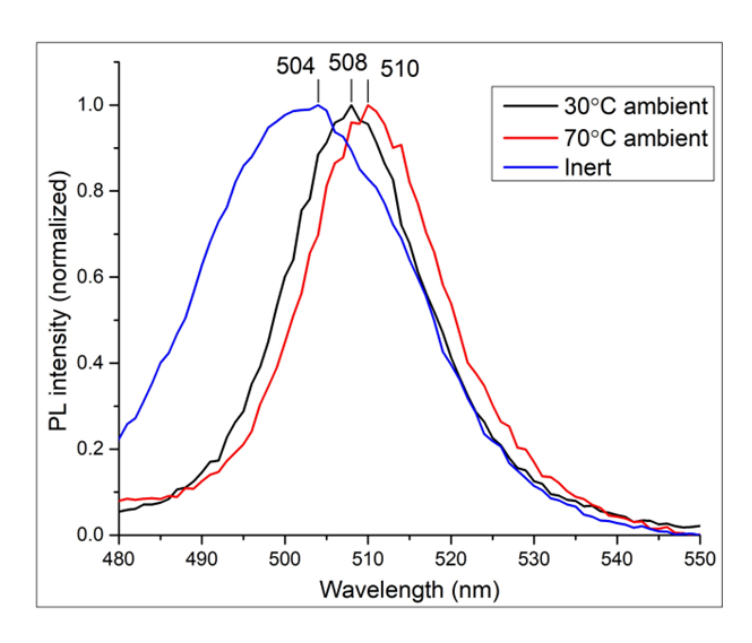


Figure 4.5: PL spectra for 30°C, 70°C and inert sample showing emission at 508nm, 510nm, and 504nm respectively.

exhibited an emission peak at 508, while the one synthesized at 70 showed a slightly red-shifted

peak at 510. Additionally, the sample synthesized under an inert atmosphere displayed a blue-shifted emission peak at 504. These shifts in PL emission suggest subtle changes in particle size, surface states, or defect density influenced by synthesis temperature and environment.

4.1.4 Time Correlated Single Photon Counting (TCSPC) results

TCSPC measurements were performed to determine the fluorescence lifetime of CsPbBr₃ quantum dots synthesized at 30 and 70. The raw PL decay data were fitted using a double exponential decay function, from which the fluorescence lifetimes were extracted.

The fitting function used is:

$$y = A_1 e^{-\frac{x}{t_1}} + A_2 e^{-\frac{x}{t_2}}$$

Here, A_1 and A_2 are the amplitudes, and t_1 and t_2 are the corresponding decay times. The average fluorescence lifetime τ is given by:

$$\tau = \frac{A_1 t_1^2 + A_2 t_2^2}{A_1 t_1 + A_2 t_2}$$

Fitting parameters									
	30°C 70°C								
	Α	В	С	D		A	В	С	D
1	Model	ExpDec2			1	Model	ExpDec2		
2	Equation	y = A1*exp(-x/t1) +	A2*exp(-x/t2) + y0	2	Equation	y = A1*exp(-x/t1) + A2*exp(-x/t2) + y0		
3	Reduced Chi-Sqr	5.79427E-6			3	Reduced Chi-Sqr	1.38252E-5		
4	Adj. R-Square	0.99934			4	Adj. R-Square	0.9985		
5			Value	Standard Error	5			Value	Standard Error
6	y offset	y0	9.83322E-4	1.08873E-4	6	y offset	y0	0.00176	4.43288E-4
7	amplitude	A1	1.00068	6.10566E-4	7	amplitude	A1	1.00641	9.07021E-4
8	decay time	t1	0.90677	0.00106	8	decay time	t1	0.93313	0.00152
9	amplitude	A2	0.02613	2.753E-4	9	amplitude	A2	0.03179	3.17061E-4
10	decay time	t2	13.60952	0.28774	10	decay time	t2	24.99936	0.96682

Figure 4.6: Fitting parameters

Based on this analysis, the average fluorescence lifetime for the quantum dots synthesized at 30 was found to be 4.45, whereas for those synthesized at 70, the lifetime increased significantly to 11.96. This increase in lifetime at higher temperature may be attributed to improved crystallinity, reduced non-radiative recombination, or enhanced surface passivation.

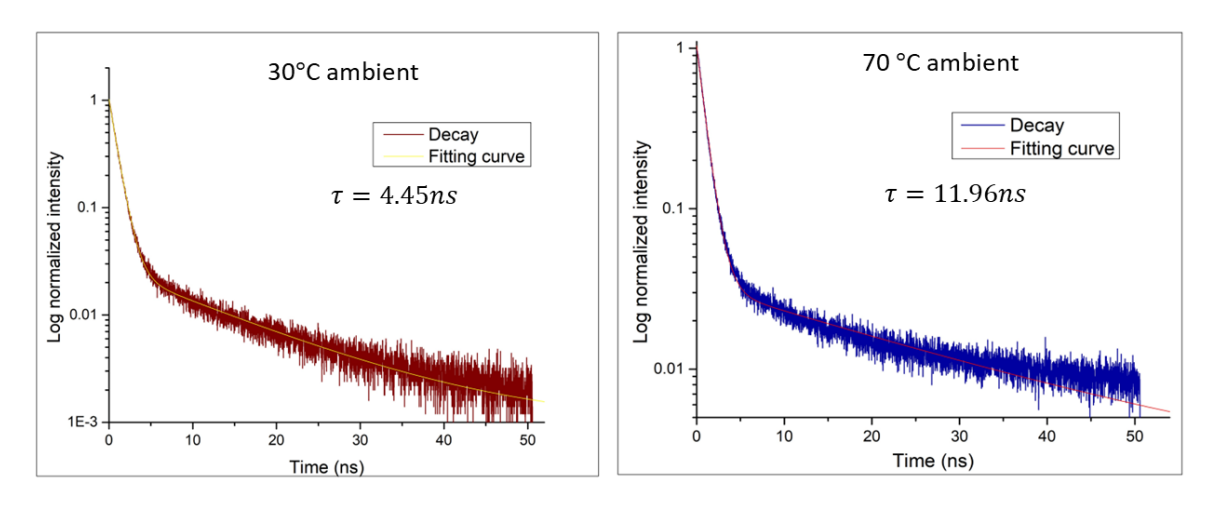


Figure 4.7: Time-resolved PL decay curve

4.2 Theoretical calculations

4.2.1 Band Gap and Quantum Dot Size Estimation

To estimate the optical band gap of the synthesized CsPbBr₃ quantum dots, Tauc plot analysis was employed. The absorption data were plotted using the Tauc relation for a direct band gap semiconductor:

$$(\alpha h\nu)^2 = A(h\nu - E_q)$$

where α is the absorption coefficient, $h\nu$ is the energy of the photon, A is a proportionality constant, and E_g is the band gap. The band gap was determined by extending the linear portion of the Tauc plot to the photon energy axis (x-axis), where $(\alpha h\nu)^2 = 0$.

After estimating the band gap, quantum dots size was calculated using the Brus equation, which relates the quantum confinement-induced band gap shift to the size of the quantum dot:

$$E(R) = E_{g,\text{bulk}} + \frac{h^2 \pi^2}{2R^2} \left(\frac{1}{m_h^*} + \frac{1}{m_e^*} \right) - \frac{1.8e^2}{4\pi \varepsilon_0 \varepsilon_r R}$$

Here:

- E(R) is the quantum dot band gap (from absorption or PL),
- $E_{q,\text{bulk}} \approx 2.3 \text{ eV}$ is the bulk band gap of CsPbBr₃,
- R is the radius of the quantum dot,

- $m_e^* = 0.12 m_0$ and $m_h^* = 0.15 m_0$, are effective mass of electron and hole, respectively with $m_0 = 9.11 \times 10^{-31}$ kg,
- $\varepsilon_r = 5.9$ is the relative dielectric constant of CsPbBr₃,
- $\varepsilon_0 = 8.854 \times 10^{-12}$ Farad/metre is the vacuum permittivity,
- $e = 1.602 \times 10^{-19}$ C represents the elementary charge,
- $h=6.626\times 10^{-34}$ Joule·sec and $\hbar=\frac{h}{2\pi}\approx 1.055\times 10^{-34}$ Joule·sec is the reduced Planck's constant.

By substituting the experimentally observed band gap E(R) into the Brus equation and solving for R, the radius (and hence the approximate size) of the quantum dots was calculated.

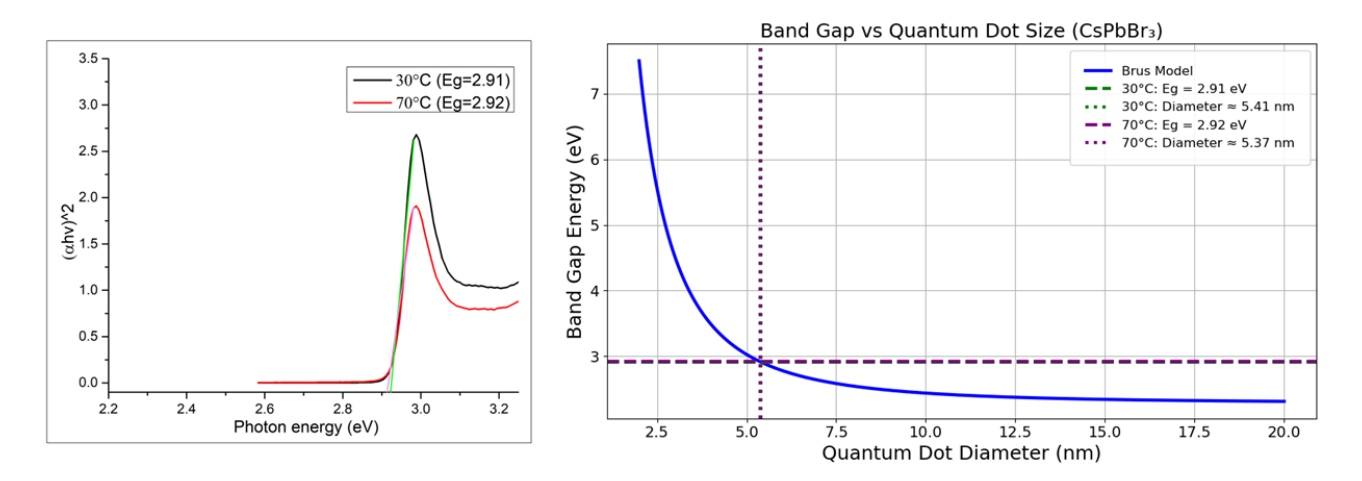


Figure 4.8: Combined Tauc and Brus plot for temperature variation

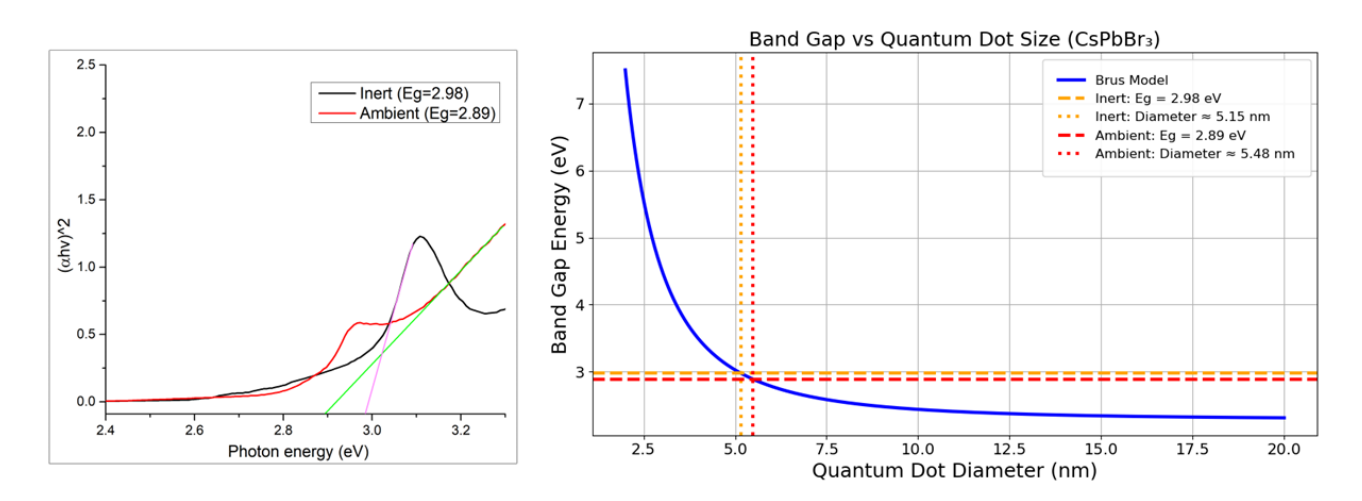


Figure 4.10: Combined Tauc and Brus plot for environment variation

The table summarizes the influence of temperature, injection method, and environment on the band gap and size of CsPbBr₃ quantum dots. The band gap varies between 2.89 and 2.98 eV, while the

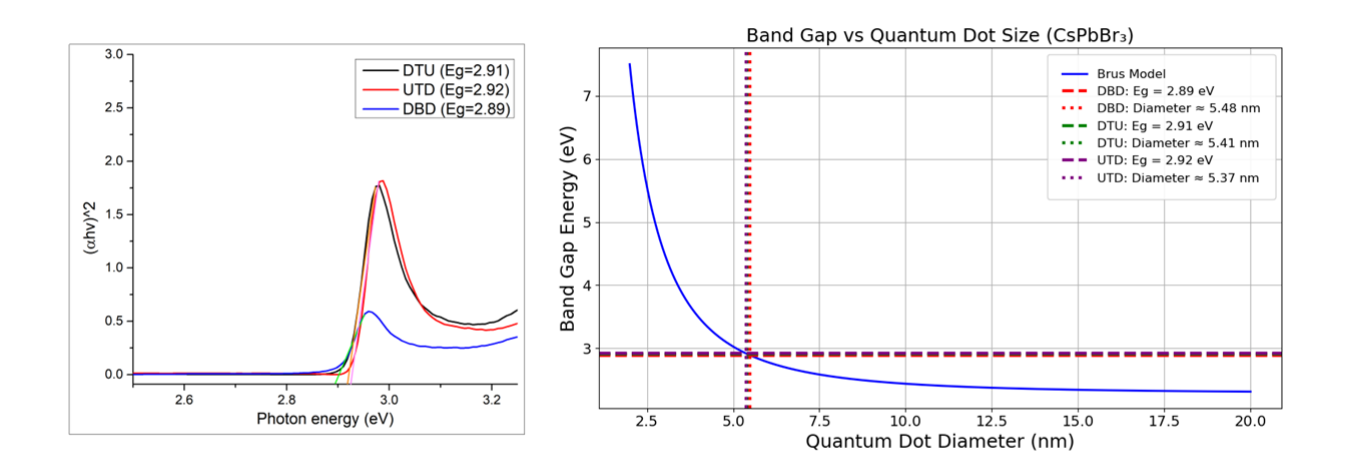


Figure 4.9: Combined Tauc and Brus plot for injection method variation

Parameter Type	Sample Description	Band Gap (eV)	Size (nm)	
Temperature Variation	Sample T1 (30°C)	2.91	5.41	
	Sample T2 (70°C)	2.92	5.37	
Injection Method Variation	Sample I1 (Burst: Up to Down)	2.92	5.37	
	Sample I2 (Burst: Down to Up)	2.91	5.41	
	Sample I3 (Drop-by-Drop)	2.89	5.48	
Environment Variation	Sample E1 (Ambient)	2.89	5.48	
	Sample E2 (Inert: Nitrogen)	2.98	5.15	

Table 4.2: Band gap and size under various synthesis conditions for CsPbBr₃ QDs.

size ranges from 5.15 to 5.48 nm. Notably, samples synthesized under an inert nitrogen atmosphere exhibit a higher band gap and smaller size.

Chapter 5

Conclusion

This thesis focused on the experimental methods to synthesize and characterize colloidal halide perovskite semiconductor nanocrystals (quantum dots), particularly CsPbBr₃, and to investigate their optoelectronic properties. A theoretical framework, such as the Brus model, was integrated with experimental results, leading to valuable insights. The primary objective was to evaluate how reaction temperature, precursor injection method, and environmental conditions influence the optical behavior of the synthesized quantum dots (QDs). Additionally, the Brus model was integrated with experimental data to estimate the size of the QDs.

We successfully synthesized CsPbBr₃ QDs under two different temperature regimes (30 °C and 70 °C), using different precursor injection techniques (DTU, UTD, and DBD), and under different environmental conditions (inert and ambient). UV–Vis absorption spectroscopy revealed distinct absorption peaks for each synthesis condition, indicating the sensitivity of band-edge features to synthesis parameters. Photoluminescence (PL) spectroscopy showed emission peaks characteristic of strong quantum confinement. TCSPC measurements provided insights into carrier dynamics, revealing different lifetimes under different synthesis conditions. These differences are attributed to variations in surface trap densities, ligand interactions, or crystallinity. The Brus equation was applied to the Tauc plot results to estimate the size of the QDs.

The combined effects of physical parameters (temperature) and process conditions (environment and injection method) play a significant role in determining the optical properties and size distribution of the QDs. These findings enhance the understanding of the relationship between synthesis parameters and QD properties, and also offer strategies to tune QD characteristics for targeted optoelectronic applications.

Despite the successful synthesis and characterization, some limitations remain. Refinement of the Brus model could improve size estimations, particularly in strongly confined systems where dielectric mismatch and non-parabolic band effects become significant. Future research should focus on optimizing synthesis parameters, investigating post-synthetic surface passivation strategies to enhance stability, and integrating these QDs into devices such as LEDs, photodetectors, and single-photon sources.

In conclusion, this study presents a comprehensive understanding of how synthesis parameters impact the optoelectronic properties of $CsPbBr_3$ quantum dots.

Bibliography

- [1] H. Fröhlich, Physica 1937, 4, 406.
- [2] A. I. Ekimov, A. A. Onushchenko, JETP Lett, 2023, 118, S15.
- [3] L. E. Brus, J. Chem. Phys. 1983, 79, 5566.
- [4] L. E. Brus, J. Chem. Phys. 1984, 80, 4403.
- [5] C. B. Murray, D. J. Norris, M. G. Bawendi, J. Am. Chem. Soc. 1993, 115, 8706.
- [6] V. M. Goldschmidt, Naturwissenschaften 1926, 14, 477.
- [7] X. Wang et al., Nanoscale Adv. 2019, 1, 1276.
- [8] L. C. Schmidt, A. Pertegás, S. González-Carrero, O. Malinkiewicz, S. Agouram, G. Mínguez Espallargas, H. J. Bolink, R. E. Galian, J. Pérez-Prieto, J. Am. Chem. Soc. 2014, 136, 850.
- [9] L. Protesescu, S. Yakunin, M. I. Bodnarchuk, F. Krieg, R. Caputo, C. H. Hendon, R. X. Yang, A. Walsh, M. V. Kovalenko, Nano Lett. 2015, 15, 3692.
- [10] R. J. Sutton, M. R. Filip, A. A. Haghighirad, N. Sakai, B. Wenger, F. Giustino, H. J. Snaith, ACS Energy Lett. 2018, 3, 1787.
- [11] D. Chen, X. Chen, J. Mater. Chem. C 2019, 7, 1413.
- [12] C. Y. Huang, H. Li, Y. Wu, et al., Nano-Micro Lett. 2023, 15, 16.
- [13] D. Yang, M. Cao, Q. Zhong, P. Li, X. Zhang, Q. Zhang, J. Mater. Chem. C 2019, 7, 757.
- [14] V. K. Ravi, G. B. Markad, A. Nag, ACS Energy Lett. 2016, 1, 665.
- [15] S. Gutiérrez Álvarez, W. Lin, M. Abdellah, J. Meng, K. Žídek, T. Pullerits, K. Zheng, ACS Appl. Mater. Interfaces 2021, 13, 44742.

- [16] G. Rainò, N. Yazdani, S. C. Boehme, et al., Nat. Commun. 2022, 13, 2587.
- [17] T. D. Kippeny, J. Chem. Educ. **2002**, 79, 1094.
- [18] X. Li, Y. Wu, S. Zhang, B. Cai, Y. Gu, J. Song, H. Zeng, Adv. Funct. Mater. 2016, 26, 2435.
- [19] K. Vighnesh, S. Wang, H. Liu, A. L. Rogach, ACS Nano 2022, 16, 19618.
- [20] M. Wahl, H.-J. Rahn, I. Gregor, R. Erdmann, J. Enderlein, Rev. Sci. Instrum. 2007, 78, 033106.